

Imaging and Etching of Self-Assembled *n*-Octadecanethiol Layers on Gold with the Scanning Tunneling Microscope

Yeon-Taik Kim and Allen J. Bard*

Department of Chemistry and Biochemistry, The University of Texas at Austin,
Austin, Texas 78712

Received September 3, 1991. In Final Form: December 2, 1991

Self-assembled monolayers of *n*-octadecanethiol on Au(111) were studied by scanning tunneling microscopy (STM). The STM images, taken with a high bias (~ 1 V) and small (~ 1 nA) tunneling current, show self-assembled monolayers with defect sites (pits). Continued scanning in this mode caused small lateral expansion of the pits and eventually a complete morphological change of the *n*-octadecanethiol-covered surface. Purposeful etching of the self-assembled monolayers could be achieved by bringing the STM probe tip closer to the substrate using a low bias potential (10 mV) and a high tunneling current (10 nA) or by the application of a high bias potential (3 V) for a few seconds. A positive substrate bias (+3 V) pulse always led to pit formation, while a negative (-3 V) substrate bias pulse produced mounds. These mounds could be removed with a positive bias pulse. The modifications induced by potential pulses were attributed to field evaporation of material from substrate or tip material. The atomic structures of etched Au surfaces using an STM tip or strong oxidizing agents, such as chromic acid and peroxide ($\text{H}_2\text{SO}_4:\text{H}_2\text{O}_2 = 7:3$) solutions, were remarkably different. The surface structure of the etched area using an STM tip showed complete distortion from the Au(111) surface, whereas peroxide solution etching preserved the original Au(111) structure.

Introduction

We describe the imaging of self-assembled monolayers of the *n*-octadecanethiol (RSH, where $\text{R} = \text{C}_{18}\text{H}_{37}$) by scanning tunneling microscopy (STM) on a gold substrate and the selective removal of RSH from the surface by tip/layer interaction. STM¹ has been used extensively to image surfaces in vacuum, air, and liquid environments and to modify surfaces (e.g., metals, graphite, semiconductors) by interaction of the probe tip with the substrate.² The possibility of using STM to fabricate patterns at the nanometer scale has been of interest in applications to the formation of nanostructures and high-resolution lithography.

Organic monolayer films on various substrates, formed by transfer from the air/water interface by the Langmuir-Blodgett (L-B) technique or by self-assembly, have been investigated extensively.³ Several reports of STM images of organic layers formed by the L-B technique have appeared⁴ and have shown that these films can be manipulated by the STM probe tip.⁵ There has been less

work done on imaging and manipulation of self-assembled monolayer films on surfaces.⁶

Experimental Section

All experiments were performed with the specimen in air with a Nanoscope II STM (Digital Instruments, Santa Barbara, CA). The films were formed on clean gold films (approximately 1500 Å thick) vacuum-evaporated (pressure less than 5×10^{-7} Torr) on a hot ($\sim 310^\circ$) mica substrate at a deposition rate of 2 Å/s.⁷ This procedure produced an atomically flat single crystal (111) surface with single crystal grain sizes as large as 100–200 nm in diameter.⁷ After preparation, the Au/mica substrate was immediately placed in a 1 mM *n*-octadecane solution in absolute ethanol for approximately 3 h at room temperature. The sample was then removed and rinsed with absolute EtOH followed by drying in a N_2 gas stream. The rinsing and drying were repeated 3 times just before the STM imaging. The Pt/Ir (80:20) tips used were mechanically cut with a wire clipper. STM images of large areas (e.g., 100 nm \times 100 nm) were obtained in the constant current (topographic) mode, and images at atomic resolution were taken in the constant height mode with a fast data acquisition rate (19–78 Hz). Self-assembly of the RSH followed previously described procedures.^{3,8} The self-assembled monolayers were imaged with the tip at a bias (V_b) of 0.5–1.0 V and tip current (I_t) of 0.5–1 nA. RSH film etching was carried out by bringing the tip closer to the film ($V_b = 10$ mV; $I_t = 10$ nA). The films could also be modified by application of a voltage pulse between tip and substrate (± 3 –5 V) for several seconds.

Results

STM Images of Freshly Prepared Au(111) Surfaces. A typical STM image of an evaporated Au(111) film on

(1) (a) Binnig, G.; Rohrer, H.; Gerber, Ch.; Weibel, E. *Phys. Rev. Lett.* **1982**, *49*, 57. (b) Avouris, P. *J. Phys. Chem.* **1990**, *94*, 2246. (c) Schardt, B. C.; Yau, S.-L.; Rinald, F. *Science* **1989**, *243* 1050. (d) Magnussen, O. M.; Hotlos, J.; Nichols, R. J.; Kolb, D. M.; Behm, R. *J. Phys. Rev. Lett.* **1990**, *64*, 2929.

(2) Quate, C. F. *Proc. NATO SCIENCE Forum '90*; Plenum Press: New York, 1991.

(3) (a) Ulman, A. In *An Introduction to Ultra-Thin Organic Films From Langmuir-Blodgett to Self-Assembly*; Academic Press: San Diego, 1991. (b) Hickman, J. J.; Ofter, D.; Laibinis, P. E.; Whitesides, G. M.; Wrighton, M. S. *Science* **1991**, *252*, 688. (c) Swalen, J. D.; Allara, D. L.; Andrade, J. D.; Chandross, E. A.; Garoft, S.; Israelachili, I.; McCarthy, T. J.; Murray, R.; Pease, R. F.; Rabolt, J. F.; Wynne, K. J.; Yu, H. *Langmuir* **1987**, *3*, 932, and references therein.

(4) (a) Smith, D. P. E.; Bryant, A.; Quate, C. F.; Rabe, J. P.; Gerber, Ch.; Swalen, J. D. *Proc. Natl. Acad. Sci. U.S.A.* **1987**, *84*, 969. (b) Smith, D. P. E.; Hober, J. K. H.; Gerber, Ch.; Binnig, G. *Science* **1989**, *245*, 43. (c) Smith, D. P. E.; Hober, J. K. H.; Binnig, G.; Nejohn, H. *Nature* **1990**, *344*, 641.

(5) Albrecht, T. R.; Dovek, M. M.; Lang, C. A.; Crutter, P.; Quate, C. F.; Kuan, S. W. J.; Frank, C. W.; Pease, R. F. *W. J. Appl. Phys.* **1988**, *64*, 1178.

(6) (a) Widrig, C. A.; Alves, C. A.; Porter, M. D. *J. Am. Chem. Soc.* **1991**, *113*, 2805. (b) Kim, Y.-T.; McCarley, R. L.; Bard, A. J., manuscript in preparation.

(7) (a) Hallmark, V. M.; Chiang, S.; Rabolt, J. F.; Swalen, J. D.; Wilson, R. J. *Phys. Rev. Lett.* **1987**, *59*, 2879. (b) Chidsey, C. E. D.; Loiacono, D. N.; Sleator, T.; Nakahara, S. *Surf. Sci.* **1988**, *200*, 45.

(8) (a) Nuzzo, R. G.; Allara, D. L. *J. Am. Chem. Soc.* **1983**, *105*, 448. (b) Bain, C. D.; Whitesides, G. M. *J. Am. Chem. Soc.* **1988**, *110*, 5897. (c) Bain, C. D.; Troughton, E. B.; Yao, Y.-T.; Evall, J.; Whitesides, G. M.; Nuzzo, R. G. *J. Am. Chem. Soc.* **1989**, *111*, 321.

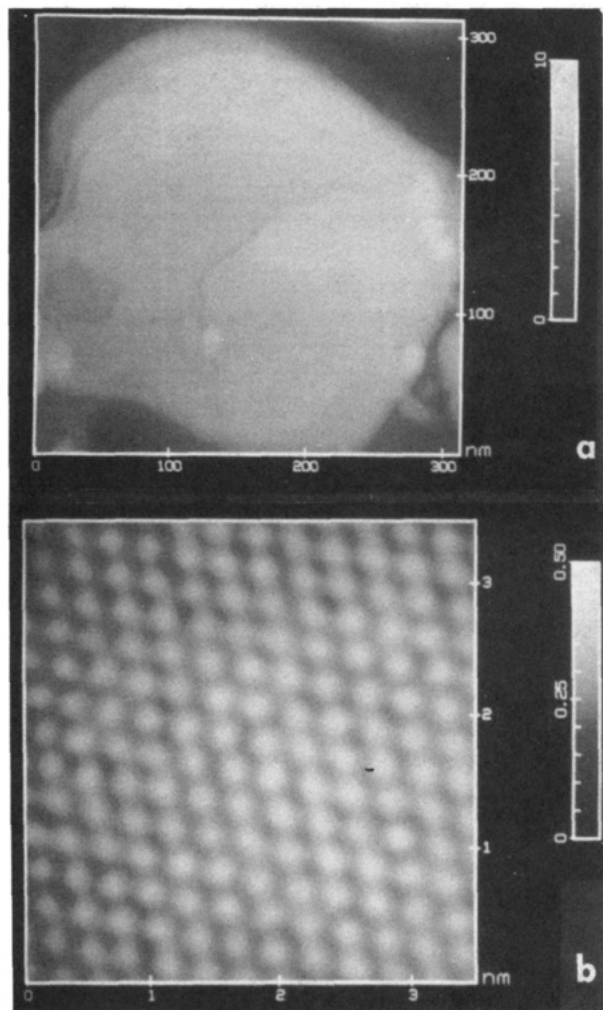


Figure 1. (a) STM image of a 310 nm \times 310 nm area of bare Au film epitaxially grown on a mica substrate (Au/mica) measured in air: constant current mode; bias (V_b) of +50 mV, tunneling current (I_t) of 10 nA. (b) STM image of a 3.5 nm \times 3.5 nm area of a bare Au/mica film: constant current mode; $V_b = +4.9$ mV; $I_t = 3.0$ nA.

mica is shown in Figure 1a. The surface is atomically flat over areas of about 100 nm \times 100 nm, as previously reported.⁷ Occasionally, rows of small gold nuclei were seen with good STM probe tips.⁹ Figure 1b shows a 35 Å \times 35 Å area with atomic resolution that corresponds to the hexagonal close packing of Au(111). The nearest and next-nearest neighbor atomic spacing is 2.9 ± 0.2 and 4.9 ± 0.2 Å, in excellent agreement with literature values for an Au(111) surface.¹⁰

STM images like those in Figure 1 were obtained within 2 days of deposition of the gold films. These samples were probably contaminated by adsorption of organic species from the air. Fresh surfaces of gold are hydrophilic, but after exposure to air for several minutes, the surfaces become hydrophobic because of adsorption of contaminants.⁸ Adsorbed organic contaminants were not seen by STM when a bare gold surface was imaged within a few days of the sample preparation. However, STM images of older gold samples, e.g., those kept in the sample container for more than 2 weeks or those deliberately contaminated by organic materials, were clearly different from freshly prepared samples. The STM image of Au

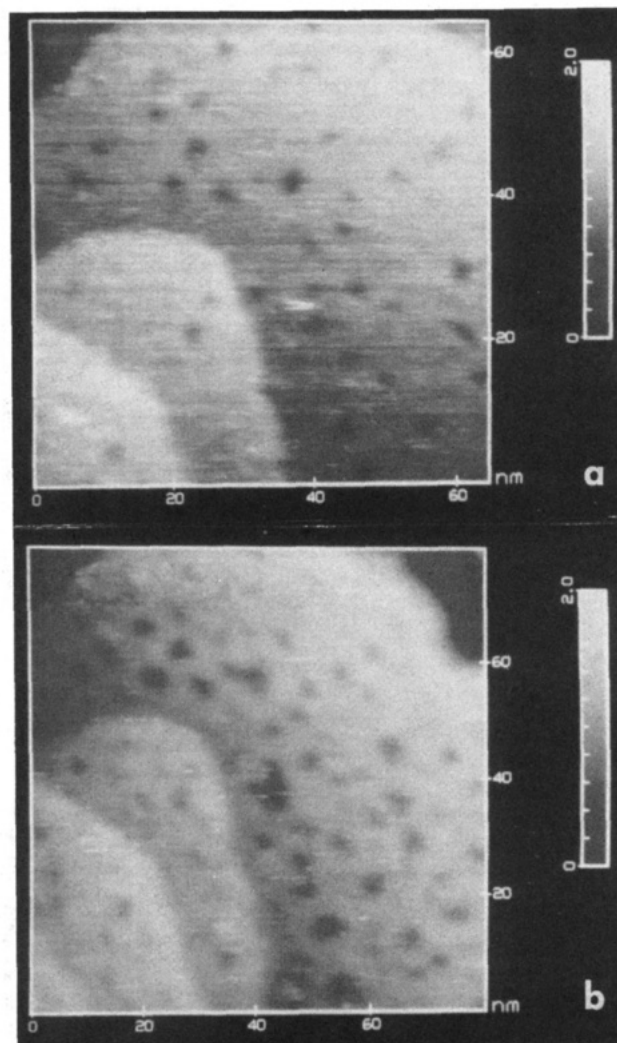


Figure 2. (a) STM image of a 65 nm \times 65 nm area of *n*-octadecanethiol film coated on Au/mica. (b) A 80 nm \times 80 nm image of the same area after 20 min of normal scanning mode operations. Images were taken in constant current mode, $V_b = +1$ V and $I_t = 1$ nA.

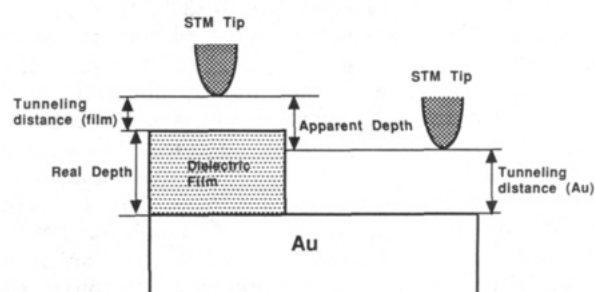


Figure 3. Schematic of STM tip positions over a bare Au and an alkanethiol chemisorbed layer.

modified with a poly(methyl methacrylate) film is discussed below.

STM Image of Freshly Prepared *n*-Octadecanethiol Films on Au(111). Self-assembled alkanethiols on Au surfaces have been characterized by many techniques (e.g., IR, LEED).^{8,11a} From these studies, alkanethiols were shown to form close-packed structures with tilt angles of approximately 30° with respect to the surface normal. Moreover, the adlattice structure of *n*-octadecanethiol on

(9) (a) Lang, C. A.; Dovek, M. M.; Nogami, J.; Quate, C. F. *Surf. Sci.* 1989, 224, L947. (b) Kim, Y.-T.; Bard, A. J. Unpublished results.

(10) Ashcroft, N. H.; Mermin, N. D. *Solid State Physics*; Saunder College: Philadelphia, PA, 1976; p 63.

(11) (a) Strong, L.; Whitesides, G. M. *Langmuir* 1988, 4, 546. (b) Chidsey, C. E. D.; Liu, C.-Y.; Rowntree, P.; Scoles, G. *J. Chem. Phys.* 1989, 91, 4421.

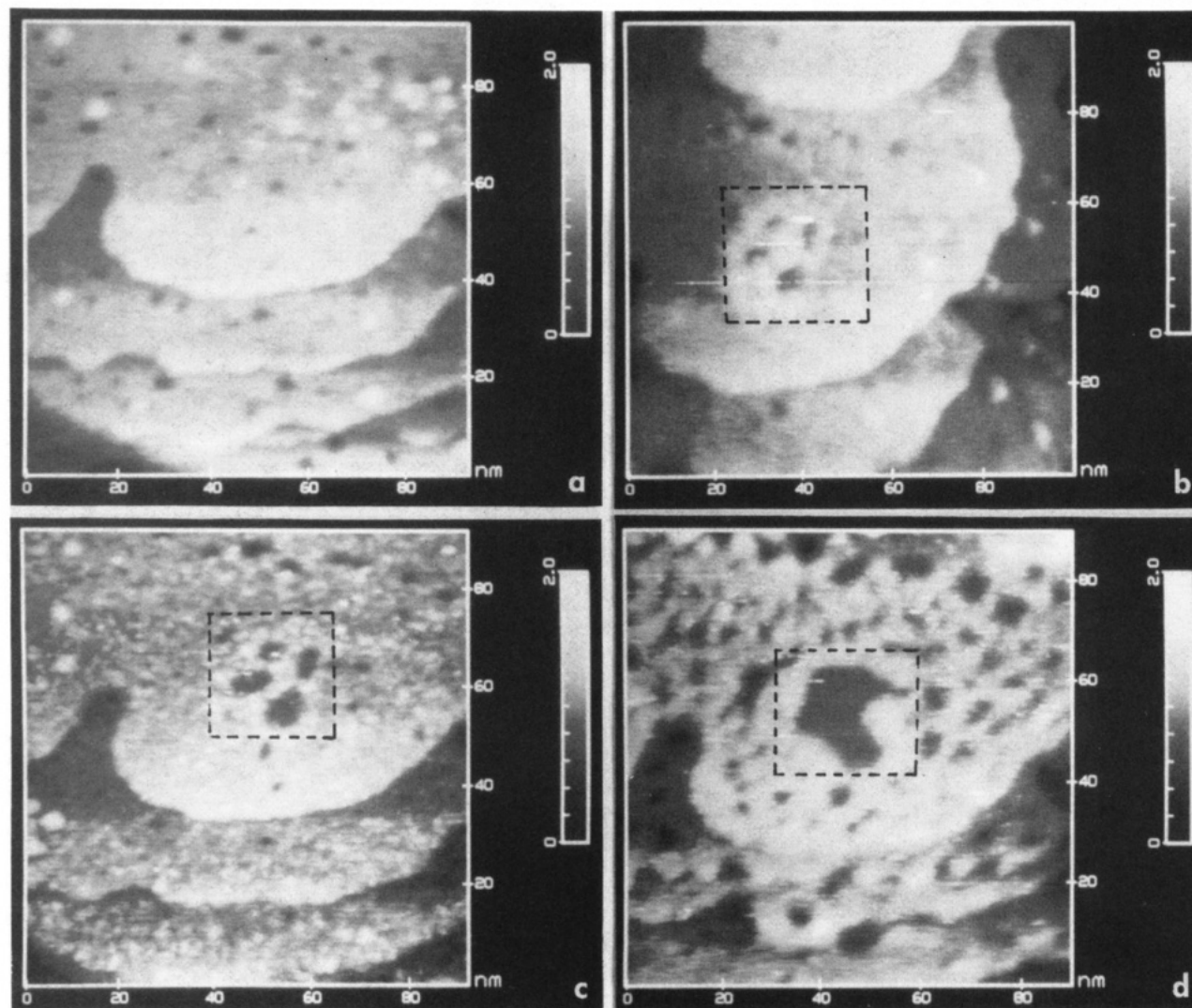


Figure 4. STM image of a 100 nm \times 100 nm (a) *n*-octadecanethiol film coated on Au/mica. (b) Same area after 10 s of etching mode ($V_b = 10$ mV, $I_t = 10$ nA) over a 10 nm \times 10 nm area (within area shown by broken line). (c) Same area after 10 min of continuous normal scanning. (d) After 35 min normal scanning. All images were taken in constant current mode, $V_b = +1$ V, and $I_t = 1$ nA.

Au was determined to be $(\sqrt{3} \times \sqrt{3})R30^\circ$.^{6,11} Figure 2a is a typical STM image of a 65 nm \times 65 nm area of an *n*-octadecanethiol covered surface. The surface generally appears uniform but with some defects (pits) and small bumps. The number and diameter of the pits varied, but the apparent depth of the pits was uniform with a value of 8 ± 1 Å, as determined from height profiles taken over many different pits on several specimens. The *z*-axis of the STM was calibrated by scans of monolayer pits in highly oriented pyrolytic graphite (HOPG) that had been oxidized in air.¹² Note that such pits were never observed for freshly prepared Au(111) surfaces. Thus, we think the pits are defects in the self-assembled layers, which might be responsible for the leakage currents observed during electrochemical measurements with film-covered electrodes.¹³ Recently Sun and Crooks reported defect structures on an *n*-octadecanethiol-covered Au(111) surface and interpreted these as nanometer scale defects contained within a self-assembled monolayer film.¹⁴ Similar defect structures of self-assembled 11-mercapto-undecanol on gold(111) and Langmuir-Blodgett films of cadmium arachidate monolayers on mica were reported.^{15,16}

A depth of 8 Å cannot be assigned to the actual monolayer thickness of *n*-octadecanethiol, which has been reported to be 20 ± 2 Å based on the molecular tilt angle measurement using infrared spectroscopy and the summation of theoretical bond lengths.⁸ A shorter chain (C_{10}) alkanethiol showed similar behavior to the C_{18} thiols but formed shallower pits (~ 5 Å). The different apparent depths of defects for the self-assembled thiols of two different lengths (C_{10} and C_{18}) suggest that the defect structures are caused by the adsorbed alkanethiol layers rather than the Au substrate. However, in all cases, the observed depths were much smaller than those expected from the chain lengths of the thiols. We explain the anomalously small apparent depth of the pits by differences in the electronic work function, or tunneling probability, of the exposed Au at the bottom of the pits and the alkanethiol film. The lower tunneling probability at the thiol film implies that the tip needs to be closer to the film than to the Au to produce a given tip current (Figure 3). Thus as one scans across a film/Au interface, the observed change in *z* will be smaller than the actual depth. Another factor in the small apparent pit depth is

(12) Chang, H.; Bard, A. J. *J. Am. Chem. Soc.* **1990**, *112*, 4598.

(13) Porter, M. D.; Bright, T. B.; Allara, D. L.; Chidsey, C. E. D. *J. Am. Chem. Soc.* **1987**, *109*, 3359.

(14) Sun, L.; Crooks, R. M. *J. Electrochem. Soc.* **1991**, *138*, L23.

(15) Häussling, L.; Michel, B.; Ringsdorf, H.; Rohrer, H. *Angew. Chem., Int. Ed. Engl.* **1991**, *30*, 569.

(16) Hansma, H. G.; Gould, S. A. C.; Hansma, P. K.; Gaub, H. E.; Longo, M. L.; Zasadzinski, J. A. N. *Langmuir*, **1991**, *7*, 1051.

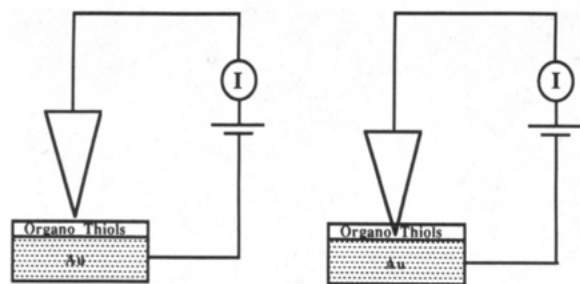


Figure 5. Proposed model for (a) normal mode and (b) etching mode.

the difference in the extent to which the Au and monolayer deform, when subjected to the forces from the tip.¹⁷ Clearly one must be cautious in relating apparent feature heights obtained by STM, especially when they involve steps between different materials, with the actual depths. The densities and diameters of the pits were not a function of the alkyl chain length in the thiols, and those found with C₁₀ were about the same as those for the C₁₈ species.

When the same area was continuously imaged ($V_b = 1$ V, $I_t = 1$ nA), interaction of the STM tip with the thiol surface appeared to initiate a slight lateral expansion of the pre-existing pits, as seen in Figure 2b. Similar etching has been found during continuous STM scanning of the surface of layered transition metal semiconductors.¹⁸ These changes in the surface under "normal" STM scanning conditions suggest significant tip/surface interactions.

Modification of *n*-Octadecanethiol Layers on Au(111). Stronger tip/surface interactions and a greater amount of etching can be obtained by bringing the tip closer to the thiol surface. The series of scans in Figure 4 shows the selective removal of organothiol surface layers by purposeful etching. Figure 4a shows an STM-imaged thiol layer on Au before etching. Figure 4b shows the same area after the STM was used in the "etching mode" ($V_b = 10$ mV, $I_t = 10$ nA, constant height mode) over four approximately 10 nm × 10 nm areas (10 s in each area); these areas are within the zone indicated by the broken line. The four holes thus produced and seen in Figure 4b reveal direct interaction between the STM tip and the thiol layers, when the STM is operated with the "etching mode". The image in Figure 4b shows that the organothiol appears to have been scratched from the surface and aggregated at the perimeter of the etched area. The effect of continued scanning (~10 and ~35 min) of the same area with normal scanning parameters is shown in parts c and d of Figure 4. As noted above, this scanning not only removes the thicker organic aggregates but also causes expansion of the pre-existing pits. The etched areas eventually connect to form the larger etched area, as seen in Figure 4d. The observed change with the "etching mode" STM parameters could not be explained by the simple uncontrollable movement of the gold edges reported by Sonnenfeld and co-workers.¹⁹ Such etching was only found with thiol-covered Au, and not with Au/mica alone. Note that Au atom movement during STM scanning has only been found with films contaminated during the evaporation process.¹⁹

We propose that the etching occurs as depicted in Figure 5. In the normal scanning mode ($V_b = 1$ V, $I_t = 1$ nA, constant current mode), the STM tip is positioned relatively far from the substrate with only a small

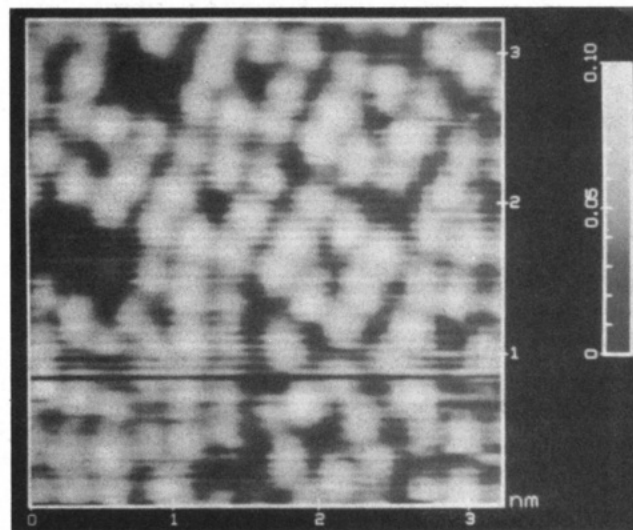


Figure 6. Unfiltered STM image of a 3.2 nm × 3.2 nm etched area of the surface shown in Figure 4d: constant height mode; $V_b = 4.6$ mV; $I_t = 25$ nA.

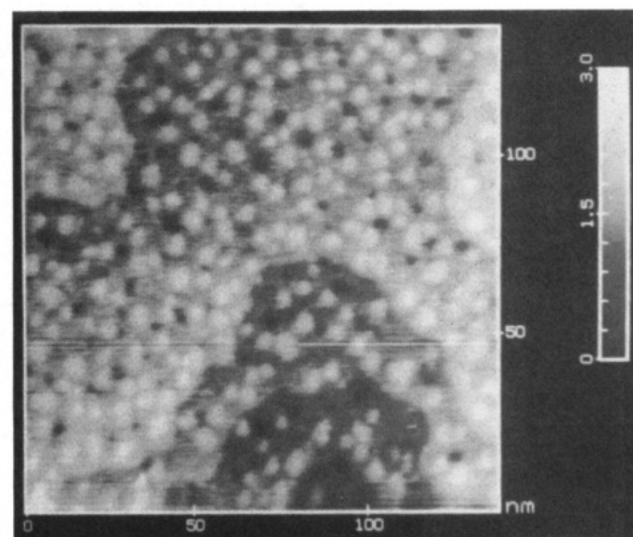


Figure 7. STM image of a 150 nm × 150 nm area of *n*-octadecanethiol film coated on Au/mica and treated with chromic acid: constant current mode; $V_b = +1$ V; $I_t = 1$ nA. The incomplete removal of thiol layers can be seen.

interaction (Figure 5a). When the bias and tunneling currents are changed to the etching mode ($V_b = 10$ mV, $I_t = 10$ nA, constant height mode) (Figure 5b), the STM tip pushes into the alkanethiol layer and can physically scratch the organic molecules off of the surface. A Langmuir-Blodgett monolayer of cadmium arachidate on mica has been removed using an atomic force microscope (AFM) with a high applied force on the tip, with the surface structure imaged afterward at a low applied force without introducing defects during scanning.¹⁶ In the "etching mode", the STM probably exerts a larger force than normal operation of the AFM ($\sim 10^{-7}$ N).

The atomic structure of Au in the etched area could be determined over a range of tunneling parameters ($V_b = 10$ –200 mV, $I_t = 2$ –30 nA). However, atomic images of the *n*-octadecanethiol layer by itself, before etching ($\sqrt{3} \times \sqrt{3}$)R30°, as reported by Porter and co-workers,^{6a} could not be observed with more than 15 different samples, although we have observed such atomic structures with 4-aminothiophenol on Au(111).^{6b} Figure 6 shows an unfiltered STM image at the bottom of an etched area of the surface shown in Figure 4d. The surface structure re-

(17) Salmeron, M.; Ogletree, D. F.; Ocal, C.; Wang, H.-C.; Neubauer, G.; Kolbe, W.; Meyer, G. *J. Vac. Sci. Technol., B* 1991, 9, 1437.

(18) Parkinson, B. *J. Am. Chem. Soc.* 1990, 112, 7498.

(19) Holland-Moritz, E.; Gordon, J., II; Borges, G.; Sonnenfeld, R. *Langmuir* 1991, 7, 301.

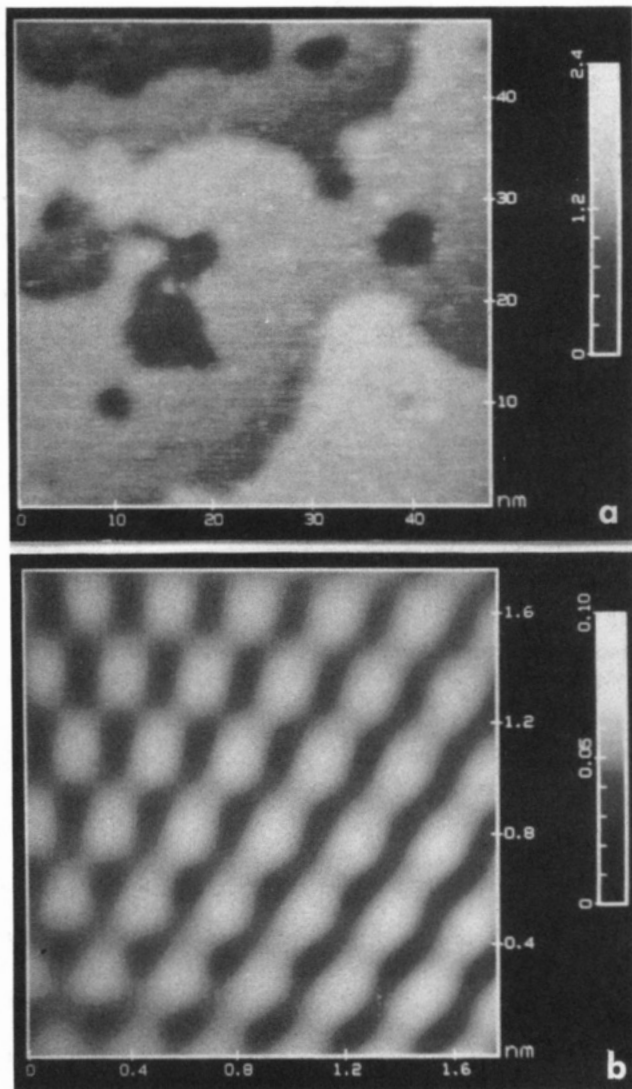


Figure 8. (a) STM image of a 50 nm \times 50 nm area of *n*-octadecanethiol film coated on Au/mica and treated with peroxide solution ($\text{H}_2\text{SO}_4:\text{H}_2\text{O}_2 = 7:3$): constant current mode; $V_b = +1$ V; $I_t = 1$ nA. Image shows complete removal of thiol layers. (b) STM image of a 17 Å \times 17 Å area of *n*-octadecanethiol film coated on Au/mica and treated with peroxide solution ($\text{H}_2\text{SO}_4:\text{H}_2\text{O}_2 = 7:3$): constant height mode; $V_b = -50.0$ mV; $I_t = 10$ nA. Complete removal of thiol layer is confirmed by Au atomic spacing. The image was spectrum filtered.

sembled neither the original Au(111) (Figure 1b) nor the $(\sqrt{3} \times \sqrt{3})R30^\circ$ structure known for the packing of *n*-alkanethiols on Au(111).^{6a,11} It probably represents a disrupted Au surface where the changes were induced by interactions between the STM tip and the substrate. The density of atoms in Figure 6 (10 atoms/nm²) is smaller than that found with Au(111) (12 atoms/nm²) but larger than the S atom density in the $(\sqrt{3} \times \sqrt{3})R30^\circ$ structure (4 atoms/nm²).

The etching of the thiol layer by the STM tip can be compared to treatment of the thiol layer with solutions of strong oxidizing agents, such as chromic acid or peroxide ($\text{H}_2\text{SO}_4:\text{H}_2\text{O}_2 = 7:3$). The *n*-octadecanethiol-covered Au(111)/mica was immersed in a chromic acid solution for 1 min. The resulting STM image (Figure 7) is characterized by small aggregates and pits, suggesting incomplete removal of the thiol layer. When the sample was treated with a peroxide solution, complete removal of the thiol layer with formation of pits in the Au was seen (Figure 8a). The treated surface showed a Au(111) structure (Figure 8b) with the same atomic spacing as in Figure 1b.

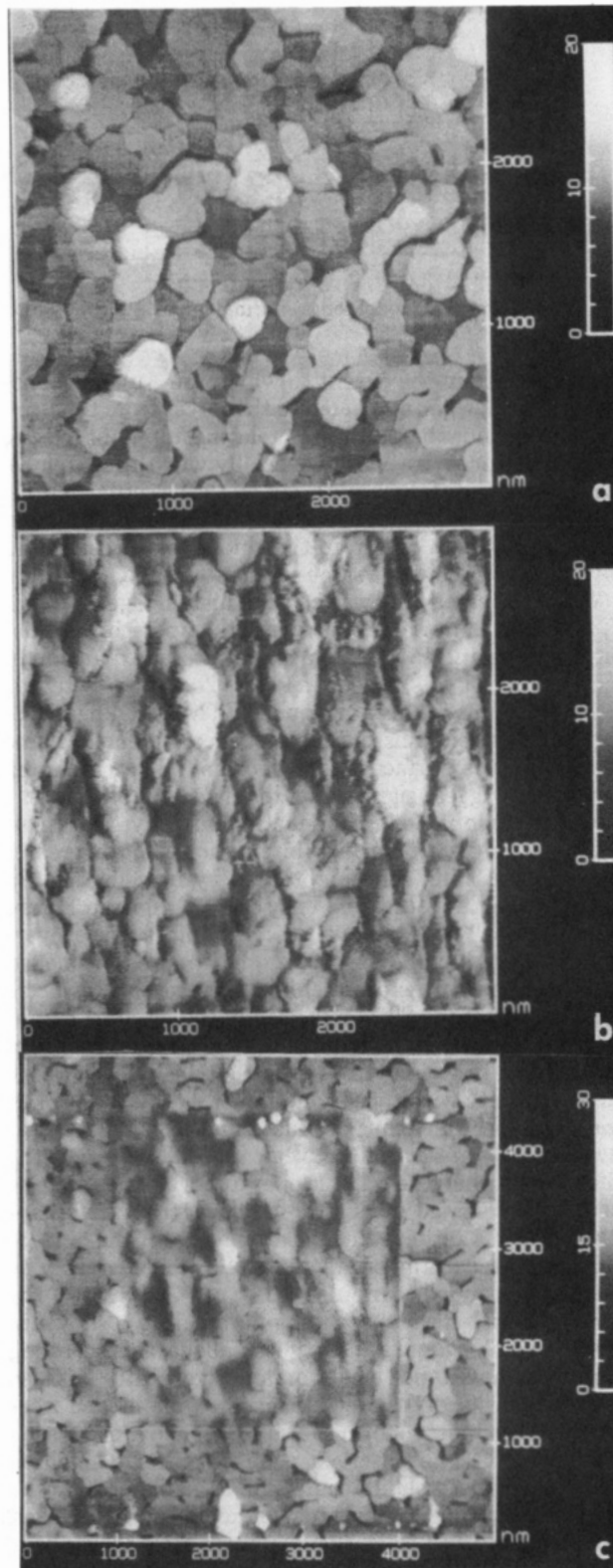


Figure 9. (a) STM image of a 3 μm \times 3 μm area of an *n*-octadecanethiol film coated on Au/mica. (b) Same area after 3 h of normal scanning mode operation. (c) 5 μm \times 5 μm around same area. All images were obtained in constant current mode, $V_b = +1$ V, and $I_t = 1$ nA.

As with the original Au(111), the image of this Au surface did not change during continuous STM scanning with normal tunneling parameters, while the thiol-covered Au showed changes in the morphology, as discussed above. The same types of pits were also seen when a bare Au substrate was treated with the peroxide solution. Thus, chemical etching with a peroxide solution not only breaks

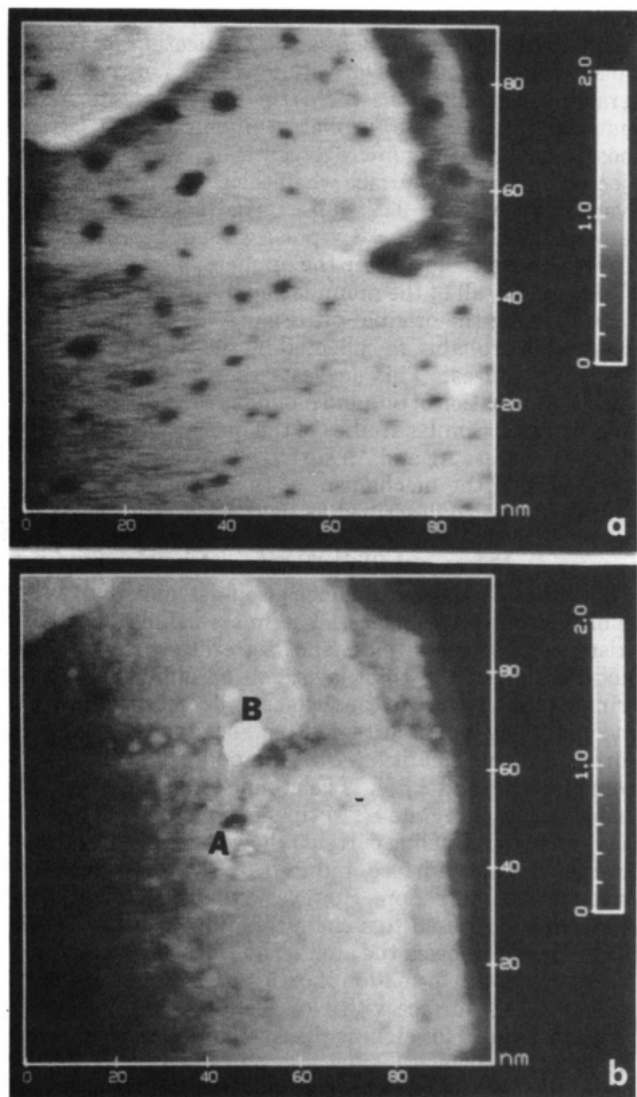


Figure 10. (a) STM image of a $100 \text{ nm} \times 100 \text{ nm}$ area of an *n*-octadecanethiol film coated on Au/mica. $V_b = +1 \text{ V}$, $I_t = 1 \text{ nA}$. (b) Same area after potential pulses. The hole caused by a $+3 \text{ V}$ bias pulse and 1 nA tunneling current is marked as A and the bump caused by a -3 V bias pulse and 1 nA tunneling current is marked as B.

Au-S bonds but leaves the surface in the Au(111) form. This can be contrasted to STM etching of the thiol-covered Au which causes a change in the Au surface, as shown in Figure 6.

Surface Modification by Extended Scanning under Imaging Conditions. Extended scanning of a larger area ($3 \mu\text{m} \times 3 \mu\text{m}$) under normal imaging conditions ($V_b = 1 \text{ V}$, $I_t = 1 \text{ nA}$) can also be used to purposely modify the thiol layer (Figure 9). Figure 9a is the first image of the *n*-octadecanethiol surface. In this large area scan, the individual grains of Au covered with RSH can be seen. After 3 h of continuous scanning, the STM image of the same area appeared different (Figure 9b). This changed STM image was not caused by fouling of the STM tip, as confirmed by scanning a larger ($5 \mu\text{m} \times 5 \mu\text{m}$) area (Figure 9c). The square ($3 \mu\text{m} \times 3 \mu\text{m}$) produced by a 3 h scan in the center changed, while the outside image of the square remained the same as that in Figure 9a. This type of change was never observed on extended scanning of freshly-prepared gold samples and, thus, is characteristic only of the RSH-coated Au, which involves strong chemical bonding between the Au substrate and the sulfur atom in the alkanethiol. Similar modifications of more weakly-

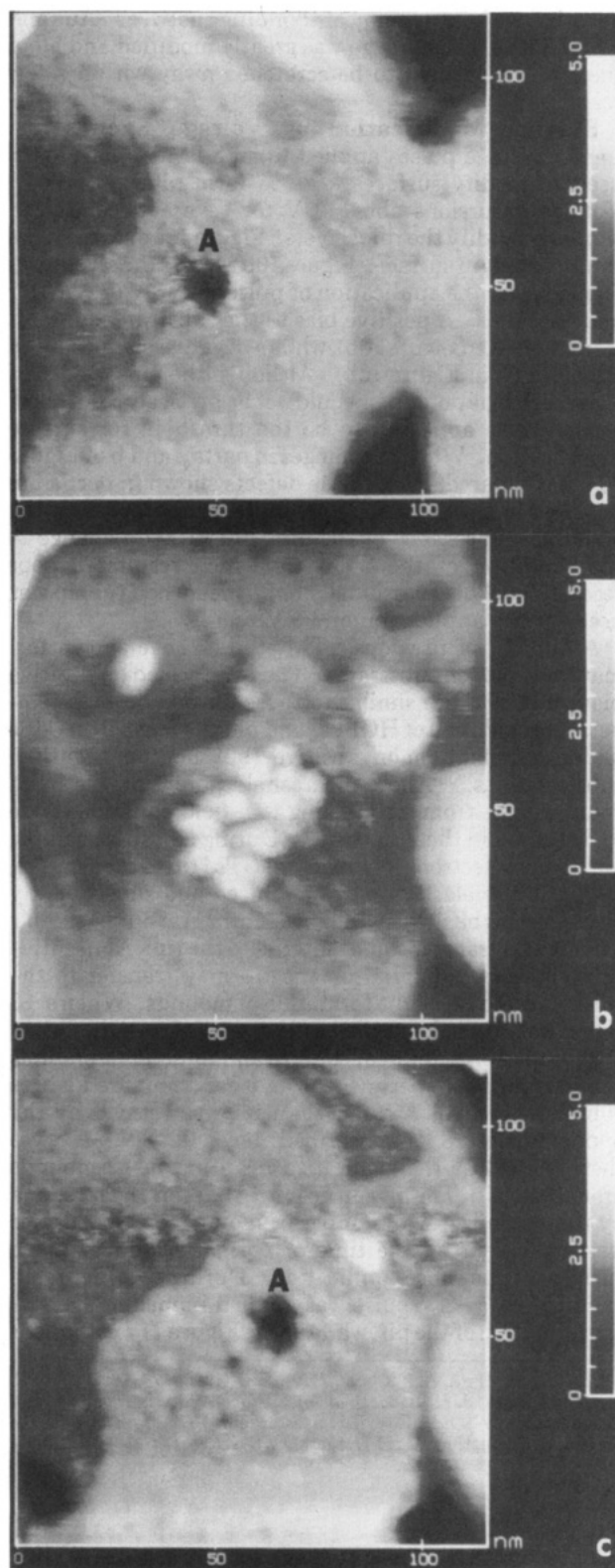


Figure 11. (a) STM image of a $120 \text{ nm} \times 120 \text{ nm}$ area of *n*-octadecanethiol film coated on Au/mica. The formation of a pit caused by the $+3 \text{ V}$ bias pulse and 1 nA tunneling current is indicated as A. (b) The formation of mounds caused by the -3 V bias pulse and 1 nA tunneling current can be seen. (c) The removal of mounds by the $+3 \text{ V}$ bias pulse and 1 nA tunneling current reveals the pit seen in (a). All images were obtained with $V_b = +1 \text{ V}$ and $I_t = 1 \text{ nA}$.

bound organic layers in much shorter times during STM scanning have been seen in preliminary experiments. For example, in the STM imaging of spin-coated poly(methyl methacrylate) (PMMA) films ($\sim 10 \text{ nm}$ thick) on Au, which

adsorbs without chemical bonding between Au and PMMA, the initial image was greatly modified and all of the PMMA seemed to be scratched away within a few scans.

Surface Modification by Voltage Excursions.

Larger voltage pulses applied to an STM tip have been used to modify surfaces, e.g., to form pits in HOPG.² Voltage excursions above 3 V for several seconds can similarly modify the thiol layers. Figure 10a shows a fresh thiol-coated Au surface. Figure 10b reveals the structures formed after the application of pulses of +3 V or -3 V for a few seconds. A positive bias to the substrate led to pit formation (A in Figure 10b), while a negative bias produced a mound (B in Figure 10b). Although the pulse width of these high bias potentials could not be precisely controlled, a ± 3 V bias appeared to be the threshold for surface modification. When the images in parts a and b of Figure 10 are compared, most of the defects shown in part a are not clear in part b. This probably does not represent the actual disappearance of the pits, but rather a change in the condition of the STM tip which results in poor resolution. This occasionally happened when the tip was used for the application of ± 3 V pulses.

A number of previous STM studies have shown formation of pits on substrates. The pits formed on positive bias on HOPG are similar to those formed on high temperature oxidation of HOPG¹² and pits are formed on CdSe under illumination on positive (but not on negative) substrate bias.²⁰ Above a threshold potential, the STM could change from a tunneling to a field emission mode as discussed in the literature.²¹ During a positive sample bias (where electrons flow from the STM tip to the sample), the surface molecules may be ionized and subsequently ejected from the surface. This can form a pit on the sample surface and transfer some material to the tip. At negative substrate bias, material on the tip may transfer to the substrate and cause the formation of mounds. When a +3 V bias was applied, one pit was always produced, but when a -3 V pulse was applied, the size and number of mounds varied from one experiment to another (compare Figures 10b and 11b). In Figure 11a, a pit was formed by the application of +3 V as described above. A -3 V pulse was then applied at the same area resulting in 12 mounds around the pit. The pit can no longer be seen and is hidden by the mounds. The number of mounds on the surface was dependent on the time of normal scanning of the surface before pulse application. During the Figure 10 experiment, a -3 V pulse was applied immediately after the formation of the pit, while in the Figure 11 experiment

the surface image was scanned for at least 10 min in the normal scanning mode before the application of a -3 V pulse. This suggests relatively longer tip/substrate interaction can allow the STM tip to accumulate more material (in this case, probably organic thiol). These loosely adsorbed organic aggregates on the tip can be ejected back to the surface when the tip material is field evaporated with a -3 V pulse. The mounds could be removed easily when a +3 V pulse was applied while the tip was above them. After the application of several +3 V bias pulses, all of the mounds had disappeared (Figure 11c), showing the original pit (Figure 11a). The mound material is probably re-collected by the STM tip during the +3 V pulses. This suggests the possibility of the selective formation of pits and mounds on the thiol-covered gold surface. Similar studies of the formation of pits and mounds on pure Ag and Au surfaces have been described recently, and the mechanism of the formation of these features was also described as field evaporation.²²

Conclusions

STM has been used to image a self-assembled alkane-thiol film on a Au surface. The imaged film shows the existence of defects (pits) and aggregates. Purposeful modification of the thiol layer can be obtained by (1) bringing the tip close to the surface by decreasing the bias and increasing the tip current, (2) extended scanning under normal imaging conditions, (3) the application of voltage excursions beyond ± 3 V. The atomic structure of a gold surface exposed by the STM tip using method (1) (a low bias and high tunneling current) showed disruption of the original Au(111) surface, induced by the STM tip and surface atom interaction. However, a thiol-covered or bare gold surface exposed to a chemical etching solution (e.g., H₂O₂-H₂SO₄) showed the atomically smooth original Au(111) surface with formation of pits. Furthermore, imaging a bare Au(111) surface with a low bias and high tunneling currents, as used for etching the thiol layers, did not alter the Au(111) surface. Thus we conclude that a direct interaction between the tip and thiol layer leads to removal of thiol and disruption of the underlying Au. Modification by this approach may be useful in high-resolution fabrication (e.g., lithography).

Acknowledgment. The support of this research by the Texas Advanced Research Program and the Robert A. Welch Foundation is gratefully acknowledged. We thank S.-L. Yau and R. L. McCarley for helpful discussions.

Registry No. Au, 7440-57-5; C₁₈H₃₇SH, 2885-00-9.

(20) Liu, C.; Bard, A. J. *Chem. Phys. Lett.* **1990**, *174*, 162.

(21) (a) Block, J. H. In *Methods of Surface Analysis Investigation*; Caanderna, A. W., Ed.; Elsevier: Amsterdam, 1975; pp 379-446. (b) Mamin, H. J.; Guethner, P. H.; Rugar, D. *Phys. Rev. Lett.* **1990**, *65*, 2418.

(22) (a) Li, Y. Z.; Vazquez, L.; Oiner, R.; Andres, R. P.; Reifenger, L. *Appl. Phys. Lett.* **1989**, *54*, 1424. (b) Rabe, J. P.; Buchholz, S. *Appl. Phys. Lett.* **1991**, *58*, 702. (c) Mamin, H. J.; Chiang, S.; Birk, H.; Guethner, P. H.; Rugar, D. *J. Vac. Sci. Technol., B* **1991**, *9*, 1398.